EVS30 Symposium
Stuttgart, Germany, October 9 - 11, 2017

Synthetic Driving Cycles-based Modelling of Extended Range Electric Vehicle Fleet Energy Demand

Branimir Škugor[1] and Joško Deur[2]

University of Zagreb, Faculty of Mechanical Engineering and Naval Architecture, Ivana Lučića 5, Zagreb, Croatia,

Email: [1]branimir.skugor@fsb.hr ; [2]josko.deur@fsb.hr

Summary

The paper deals with modelling of transport energy demand related to an electric vehicle (EV) fleet. The main aim of the paper is to provide a proper methodology of deriving a simple transport energy demand model aimed to be used within: (i) real-time control of EV fleet charging, (ii) planning of EV fleet routes, and (iii) various EV fleet-related techno-economic analysis studies. The model is represented by maps also known as response surfaces, which are obtained by simulating the considered EV model over synthetic driving cycles. The synthetic driving cycles are introduced to replace a high number of recorded driving cycles in a statistically representative way, thus reducing the number of time-consuming EV simulations. The final transport energy demand model is validated against the more precise energy consumption data obtained by simulating EREV model over the full set of recorded driving cycle.

Keywords: energy consumption, modelling, EREV (extended range electric vehicle)

1 Introduction

There is a growing tendency of developing new business models and charging technologies related to electric vehicles (EV), as EVs start appearing on roads in more significant numbers. Since vehicles are parked most of the time, EVs become available to serve as a controllable load and to provide its battery capacity as an electrical storage to the grid. In this way, an EV fleet comprising a high number of EVs can participate in different electricity markets (e.g. for load levelling, spinning reserves and similar), with an aggregator serving as an interface, in order to obtain different benefits such as lowering charging cost. However, in order to satisfy different, possibly conflicting objectives and constraints which can occur in such complex transport-energy systems, advanced information and communication technologies along with advanced optimisation algorithms should be used. Since an EV fleet can include a high number of EVs, a transport energy demand model used within a charging optimisation algorithm on the aggregator level should be simple, computationally efficient and of satisfying accuracy. This is particularly important for real-time charging management applications, where the charging optimisation algorithms are executed on line.

To this end, transport energy demand modelling based on response surfaces is elaborated in this paper. In [1], this approach is proposed for the assessment of plug-in hybrid electric vehicles (PHEV) impact on the grid. The same methodology is used in [2] to derive an EREV fleet energy demand model aimed to be used within a bi-level charging management framework. In both papers, PHEV/EREV models are simulated

over representative synthetic driving cycles for a wide range of initial battery state-of-charge values (SoC_{init}, i.e. SoC at the beginning of the driving cycle). The synthetic driving cycles are used instead of a high number of recorded driving cycles in order to reduce the needed number of simulations and correspondingly to reduce the simulation time [3, 4].

The main aim of this paper is to provide a straightforward methodology for the response surface-based modelling of transport energy demand, which also includes an exhaustive validation of the obtained models. The number of combinations of synthetic driving cycles and initial SoC values, and correspondingly the number of needed EREV model simulations, is minimised in order to simplify and accelerate the process of building the transport energy demand model of satisfying accuracy. The proposed methodology is demonstrated for the case of delivery vehicle fleet of a local retail company, whose vehicles are virtually replaced with EREVs.

The main contributions of this paper with respect to the previous relevant publications [1-4] are as follows: (i) novel single parameter-based validation of synthetic driving cycles used for deriving a transport energy demand model; (ii) validation of the obtained transport energy demand model against more complex one based on simulation of the EV fleet over the recorded driving cycles; (iii) novel mapping of synthetic driving cycles-based simulation results, where the transport energy demand maps of the desired resolution with respect to travelled distance can be achieved, while keeping the low number of synthetic driving cycles used; and (iv) demonstration of the novel application of synthetic driving cycles for all electric range (AER) estimation.

2 Modelling of extended range-type delivery electric vehicle

This section first provides a brief description of the particular delivery vehicle fleet consisting of conventional vehicles which are considered for electrification. Then, a model of extended range electric vehicle (EREV), aimed at replacing the conventional delivery vehicle, is briefly described and simulated over recorded driving cycles. Details about the considered delivery vehicle fleet and the corresponding driving data collection are given in [4], while the details about modelling of the conventional and electric delivery vehicles are given in [5].

2.1 Delivery vehicle fleet description and driving cycle data collection

The delivery vehicle fleet of a local retail company is considered in this paper to serve as a case study for the demonstration of the proposed methodology. The mission of delivery vehicles is to transport cargo from the main distribution centre to the sales centres. Ten mid-size delivery vehicles are selected as a fleet representative since they cover both inner-city as well as inter-city driving missions. The selected delivery vehicles are of type MAN-TGM 15.240, with the loading capacity of 7460 kg and the empty vehicle mass of 7860 kg, and propelled by a diesel engine with the maximum power of 176 kW. The vehicle maximum velocity is limited to 90 km/h.

The driving data were being recorded for the 10 vehicles continuously during 24-hour periods over three months (91 day) by using GPS and GPRS data recording equipment with the sampling time of 1 second. The recorded GPS data include: vehicle ID number, time stamps, GPS longitude and latitude positions, vehicle velocity, and elevation; while the recorded CAN data include: engine rotation speed and cumulative fuel consumption. The recorded data are separated into driving cycles, where one driving cycle starts when a vehicle departures from the distribution centre and ends when the same vehicle arrives back to the distribution centre, thus finishing its driving mission. This procedure resulted in total of 2286 driving cycles recorded.

2.2 Modelling of delivery extended range electric vehicle

The existing conventional vehicle is modelled and validated against experimental data in [5]. A model of fully EV of comparable torque and power characteristics is built up in the same reference, and then extended in [2] with a sub-model of a range extender (an internal combustion engine (ICE) and a generator combined with the EV drivetrain) in a series hybrid powertrain configuration. In this way, an extended

range electric vehicle (EREV) model capable of satisfying the range of each recorded driving cycle is obtained. In this type of powertrain configuration, the propulsion power is provided only by the main electric motor, while the range extender is used for battery charging in order to sustain the battery charge and consequently to extend the range.

Fig. 1 represents the block diagram of the backward-looking EREV model, where the demanded torque and speed on wheels, τ_L and ω_L, are calculated from the vehicle velocity v_v and acceleration dv_v/dt as follows (the block *Driver demand* in Fig. 1a)

$$\tau_L = r\left[\underbrace{m_v dv_v/dt}_{\text{Acceleration force}} + \underbrace{m_v g\sin\alpha}_{\text{Uphill driving force}} + \underbrace{m_v g R_o\cos\alpha}_{\text{Rolling resistance force}} + \underbrace{0.5\rho_{air}C_d A_f v_v^{\,2}}_{\text{Aerodynamic resistance force}}\right], \tag{1}$$

$$\omega_L = v_v / r, \tag{2}$$

where m_v is the combined vehicle and cargo mass, r is the effective tire radius, g is the gravitational acceleration, α is the road slope, R_o is the tire rolling coefficient, ρ_{air} is the air density with the standard value of 1.225 kg/m^3, C_d is the vehicle aerodynamic drag coefficient, and A_f is the vehicle frontal cross section area.

The relations between speeds and torques of the main electric motor (ω_m, τ_m) and wheels (ω_L, τ_L) are determined by the following kinematic equations (the block *Mechanical transmission* in Fig. 1a)

$$\omega_m = i_o h\omega_L = i_o h\frac{v_v}{r}, \tag{3}$$

$$\tau_m = \frac{\tau_L}{\eta_t i_o h}, \tag{4}$$

where i_o is the fixed final drive gear ratio, h is the transmission gear ratio, and η_t is the drive train efficiency. The transmission ratio h is assumed to take two values (two-speed transmission). The ICE fuel consumption and electric machine efficiencies are modelled by using 2D maps, while the corresponding maximum torque curves are modelled by using 1D maps (see illustrations in the corresponding blocks in Fig. 1a). The torque and speeds of the ICE motor (ω_e, τ_e) and the generator (ω_g, τ_g) are coupled together through the single ratio transmission, characterised by the gear ratio h_G (see Fig. 1a).

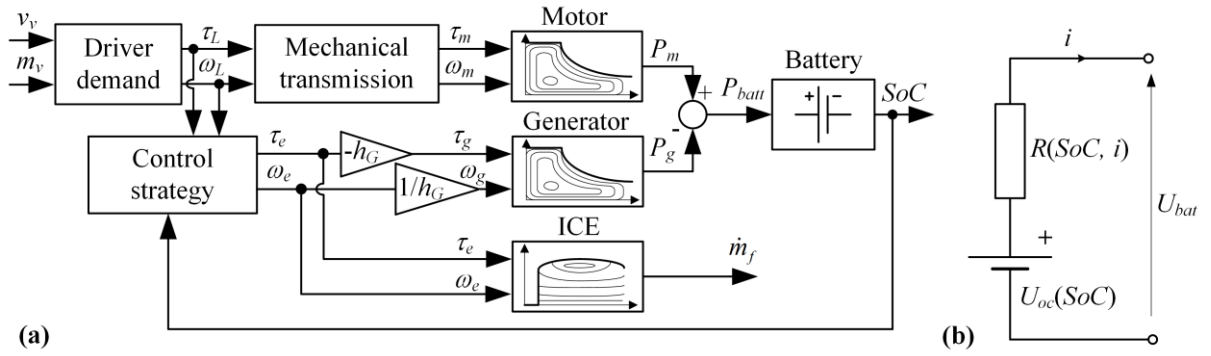

Figure 1: Block diagram of quasi-static (backward) model of EREV truck powertrain (a), and equivalent battery circuit (b).

The battery is modelled as a SoC-dependent open-circuit voltage source and internal resistance (see Fig. 1b). The following nonlinear differential equation describes the battery model dynamics

$$\dot{SoC} = \frac{\sqrt{U_{oc}^2(SoC) - 4R(SoC,i)P_{batt}} - U_{oc}(SoC)}{2Q_{\max}R(SoC,i)}, \tag{5}$$

where state-of-charge (SoC) is the state variable which can takes values between 0 and 1 (0 corresponds to the fully discharged battery, and 1 to the fully charged battery), P_{batt} is the battery power, U_{oc} is the battery

open-circuit voltage, R is the internal resistance, and Q_{max} is the battery capacity. The battery power P_{batt} is determined by electrical powers of electric motor and generator (see Fig. 1a). The capacity Q_{max} and mass of one battery cell equals to 15.9 Ah and 0.63 kg, respectively. The number of battery cells equals to 1300, which results in approximately 73 kWh of the total battery capacity, and the battery mass of 819 kg.

The control strategy sets the powertrain to operate in the charge depleting (CD) regime, where only the main electric motor is used for vehicle propulsion until the battery SoC falls to some predefined low value (here, it is set to 0.3). The operation is switched to the charge sustaining (CS) regime, where the range extender is activated in order to sustain the battery SoC (at the reference value of 0.3). The range achieved in the CD regime until switching to the CS regime is referred to as all electric range (AER), since in this regime only electric energy from the battery is used to propel a vehicle via the electric motor. The CS regime control strategy is such that it on-line optimises the ICE operating point (ω_e, τ_e) with the aim to minimise the equivalent fuel consumption. This instantaneous optimisation-based control strategy is known as equivalent consumption minimisation strategy (ECMS), and it is combined with rule-based (RB) control strategy which includes: ICE on/off switching logic, SoC controller, and ICE operating point setting functionality. By having the explicit SoC controller within the control strategy, the sustainability of battery SoC is guaranteed [6]. The abbreviation RB+ECMS is used for the final powertrain control strategy. Details about the RB+ECMS control strategy are given in [7].

By using the developed EREV model and the corresponding RB+ECMS control strategy, the simulations are conducted over all recorded driving cycles for the sake of preliminary analysis. For this purpose, the initial battery SoC is set to 0.3 in order to switch to the CS regime immediately by the start of simulation. This resulted in 2286 simulations with the total simulation time of 4.5 hours (the simulations conducted in Matlab Simulink environment). The vehicle mass m_v is set to the constant value of 10066 kg for each driving cycle, which corresponds to the vehicle carrying the average cargo mass. Since the geographic area where the vehicles operate is mostly flat, the road slope impact in Eq. (1) is neglected (α is set to 0). Further, the cumulative driving cycle energy is defined for the purpose of driving cycle analysis:

$$E_{dc} = \int_{t=0}^{t_f} \tau_L \omega_L dt \,, \tag{6}$$

where t_f denotes the total time of a driving cycle. The mean specific driving cycle energy per km of travelled distance $\overline{E}_{dc}$ (J/km) is then calculated by dividing the total driving cycle energy E_{dc} with the total distance travelled d.

Fig. 2 shows the graphical relation of the simulated fuel consumption V_f with respect to driving cycle energy E_{dc} (Fig. 2a) and with respect to travelled distance d (Fig. 2b), along with the corresponding values of correlation coefficients (K) between these variables (K = 1 denotes the full correlation, while K = 0 denotes no correlation between input variables; Matlab function *corrcoef*(.) is used to calculate the correlation coefficients). The almost full correlation between E_{dc} and V_f (K = 0.9997; Fig. 2a) means that the driving cycle energy is very significant variable from the perspective of energy (i.e. fuel) consumption. Therefore, the energy consumption-related characteristics of driving cycles can be analysed via analysis of E_{dc} (i.e. without conducting the time-consuming simulations), e.g. for the purpose of clustering the

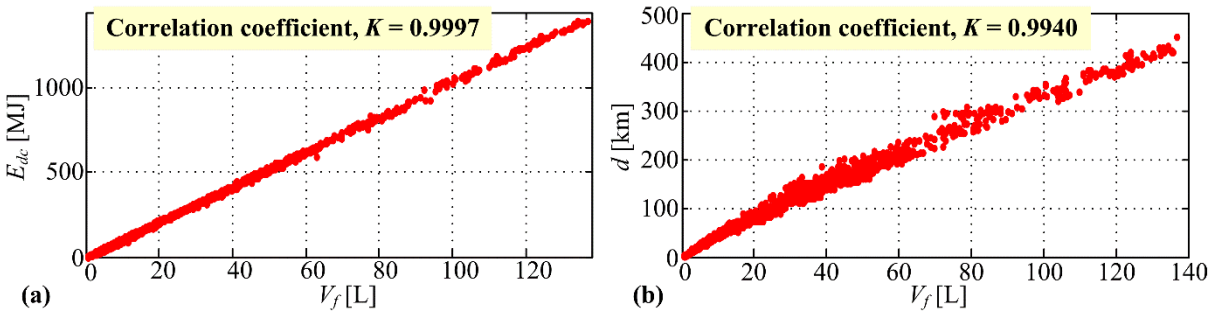

Figure 2: Cumulative energy on the wheels E_{dc} (a) and travelled distance d (b) with respect to fuel consumption V_f for the case of recorded driving cycle-based simulations (K – correlation coefficient; the initial SoC for each driving cycle was set to 0.3).

recorded driving cycles. Slight deviation from the full correlation in this case can be explained by the nonlinearities in the powertrain components characteristics (from fuel tank to wheels), e.g. ICE fuel consumption map, efficiency maps of electric machines, battery dynamics etc. Further, very high correlation between the travelled distance d and the fuel consumption V_f and (Fig. 2b) implies that the recorded driving cycles can be clustered with respect to the travelled distance, as well (this approach is elaborated in more details in the next section). Slight deviations from the full correlation are caused by the nonlinearities in the longitudinal vehicle dynamics equation (see Eq. (1)) in addition to the nonlinearities to the powertrain components characteristics.

3 Synthetic driving cycles

The motivation for developing synthetic driving cycles is to replace a large set of recorded driving cycles with a several statistically representative cycles, thus significantly reducing the number of required time-consuming simulations required by the transport energy demand modelling procedure. This section describes the driving cycle synthesis for the case of delivery vehicle fleet presented in the previous section. The synthesis procedure is based on Markov chain methodology [4, 3] and is divided into three main steps [4]: (i) clustering of recorded driving cycles, (ii) calculation of transition probability (TP) matrices for each cluster, and (iii) generation and validation of synthetic driving cycles for each cluster. The final number of synthetic driving cycles correspond to the number of clusters, i.e. a single driving cycle is synthesized for each cluster.

3.1 Clustering of recorded driving cycles

According to the finding that the total energy (i.e. fuel) consumption highly correlates with the travelled distance (Fig. 2b), the recorded driving cycles are clustered with respect to this criterion by using the in-built Matlab function *kmeans*(.). The clusters of recorded driving cycles are shown in Fig. 3a in terms of specific driving cycle energy vs. travelled distance plot. The resulting boundaries between clusters in terms of travelled distance are 49.6 km, 121.4 km, and 247.9 km. It can be seen that the specific energy increases with the travelled distance, which can be explained by the higher average vehicle velocity for the case of larger travelled distance (see the distribution of specific energy and mean velocities over clusters, given in Table 1), and, thus, progressively higher aerodynamic resistance (see Eq. (1)). Based on the assumption that the specific energy is a critical parameter for the transport energy demand models accuracy (see Subsection 3.3 for confirmation of this assumption), the following criterion is used for choosing the optimal number of driving cycle clusters (TSEE = Total Specific Energy Error)

$$TSEE = \sum_{i=1}^{N} \sum_{j=1}^{M_i} \left| \overline{E}_{dc,i,j} - \overline{E}_{dc,mean,i} \right|, \tag{7}$$

where N is the number of clusters, M_i is the number of driving cycles within i^{th} cluster, $\overline{E}_{dc,i,j}$ is the specific energy of the j^{th} recorded driving cycle within the i^{th} cluster, and $\overline{E}_{dc,mean,i}$ is the mean specific energy

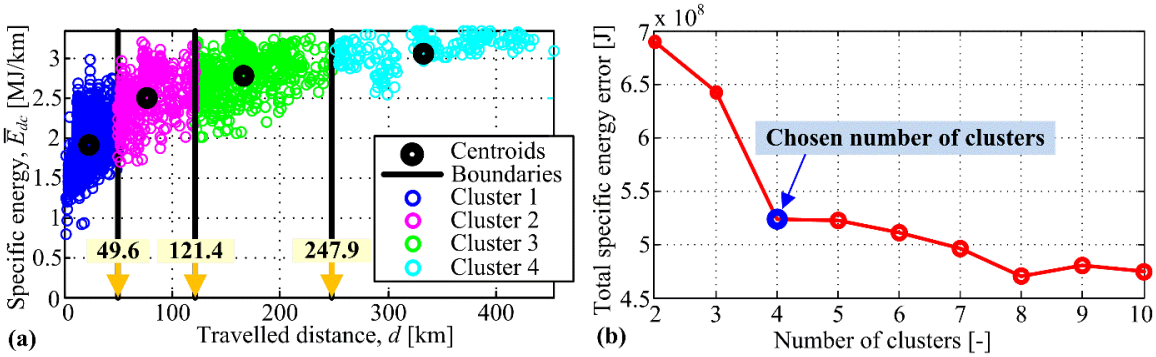

Figure 3: Distribution of specific energy on wheels with respect to travelled distance over selected clusters (a), and total specific energy error (TSEE) with respect to number of driving cycle clusters (b).

within the i^{th} cluster. Fig. 3b shows the dependence of TSEE criterion with respect to the number of clusters. The aim is to choose a minimal number of clusters, while achieving a relatively low value of TSEE criterion. In the particular case, four clusters of driving cycles are selected (denoted with different colours in Fig. 3a), because further increase of number of clusters does not reduce TSEE criterion significantly (see Fig. 3b).

Table 1: Statistics of recorded driving cycles related to specific energy, velocity and acceleration over selected clusters.

	Specific energy [MJ/km]				**Velocity [km/h]**		**Pos. acc. [m/s^2]**		**Neg. acc. [m/s^2]**	
	Min	Mean	Max	Std	Mean	Std	Mean	Std	Mean	Std
Cluster 1	0.79	**1.91**	2.98	0.33	**39.5**	23.8	**0.40**	0.36	**-0.40**	0.43
Cluster 2	1.70	**2.53**	3.20	0.30	**55.5**	26.4	**0.32**	0.32	**-0.32**	0.39
Cluster 3	2.01	**2.81**	3.29	0.26	**63.8**	26.0	**0.26**	0.29	**-0.27**	0.35
Cluster 4	2.54	**3.10**	3.34	0.18	**74.5**	22.4	**0.20**	0.26	**-0.21**	0.31
Total	0.79	**2.77**	3.34	0.53	**60.6**	27.4	**0.28**	0.32	**-0.29**	0.37

3.2 Synthesis and validation of driving cycles

The first step after recorded driving cycles clustering is to define a finite number of discrete values of vehicle velocity and vehicle acceleration. All combinations of velocity- and acceleration-related discrete values define the set of all possible states of Markov chain. The probability of transition between two Markov chain states are defined as

$$p_{qr,ij} := P(X_{k+1} = a_i, v_j \mid X_k = a_q, v_r),\ \Pi_{qr} := (p_{ij}), \tag{8}$$

where $p_{qr,ij}$ denotes the probability of transition from the current state (a_q, v_r) in the k^{th} discrete time step to the state (a_i, v_j) in the next k+1th discrete time step. All transition probabilities are organised into the transition probability matrix (TPM; Π_{qr} is the matrix which contains transition probabilities from the state denoted with indices q and r to all other states). TPM is parameterised based on the transitions between velocity- and acceleration-related states observed in the recorded data by using the maximum likelihood approach: the transitions between states are first counted and stored in TPM, and afterwards normalised in order to represent probabilities.

TPMs are calculated for each cluster of driving cycles shown in Fig. 3a, and 50 synthetic driving cycles (which is shown to be enough) for each cluster are generated by using random number generator and the corresponding TPM (more details on generating the synthetic driving cycles are given in [4]). In accordance to the clusters' boundaries (Fig. 3a), the target distance d of synthetic driving cycles for Cluster 1 is set to 49.6 km, for Cluster 2 to 121.4 km, for Cluster 3 to 247.9 km, and for Cluster 4 to 450 km. Then, the simulations of EREV model are conducted over all synthetic driving cycles for the case of initial SoC value set to the fixed value of 0.3 for the sake of preliminary analysis and synthetic driving cycles validation. The simulation results include the fuel consumption V_f and the final SoC SoC_{end} versus travelled distance d with very high resolution. The prediction of V_f and SoC_{end} for the particular travelled distance d can be obtained by the means of linear interpolation of the simulation results (the simulation results whose travelled distance range includes the considered travelled distance d are used and interpolated, e.g. if the travelled distance is within 0 and 49.6 km, the simulation results related to the synthetic driving cycle from Cluster 1 are used for the fuel consumption prediction and the final SoC).

The following mean absolute error (MAE) index is introduced in order to quantify the accuracy of predicting the fuel consumption by simulating the EREV model over generated synthetic driving cycles for the sake of validation.

$$MAE_1 = 100 \cdot \frac{\sum_{j=1}^{M_j} \left| V_{f,model}(d_j) - V_{f,rec,j} \right| / V_{f,rec,j}}{M_j} \ [\%]. \tag{9}$$

In Eq. (9), M_i is the total number of recorded driving cycles within i^{th} cluster, $V_{f,model}$ is the predicted synthetic driving cycle-based fuel consumption which depends on the travelled distance d (the simulation results of the synthetic driving cycle from the corresponding cluster are used for the fuel consumption prediction), d_j is the travelled distance of the j^{th} driving cycle, and $V_{f,rec,j}$ is the fuel consumption obtained by the simulation of EREV model over j^{th} recorded driving cycle within i^{th} cluster. The accuracy of predicting the SoC-at-destination, SoC_{end}, is calculated in a similar way:

$$MAE_2 = 100 \cdot \frac{\sum_{j=1}^{M_i} \left| SoC_{end,model}(d_j) - SoC_{end,rec,j} \right| / SoC_{end,rec,j}}{M_i} \,[\%]. \tag{10}$$

In this preliminary analysis only the accuracy of predicting the fuel consumption MAE_1 is analysed, since the initial SoC is set to the fixed value of 0.3, and the final SoC (SoC_{end}) is then assumed to take the same value (because of CS regime which intends to sustain the SoC around the target value of 0.3).

Fig. 4 shows the distribution of indices MAE_1 with respect to driving cycle specific energy for the case of 50 synthetic driving cycles within each cluster, along with the mean specific energy of the corresponding recorded driving cycles (straight lines; see also Table 1). By analysing the distribution of synthetic driving cycles-related results, the trend of increase in the model error MAE_1 with the deviation of its specific energy from the corresponding mean value can be observed (slight variations from this trend can be explained by the fact that the final SoC values at the end of driving cycles are not strictly the same for different driving cycles). This confirms the assumption that the mean specific driving cycle energy is the critical parameter for the model accuracy and justifies the approach of synthetic driving cycles validation based on this single parameter.

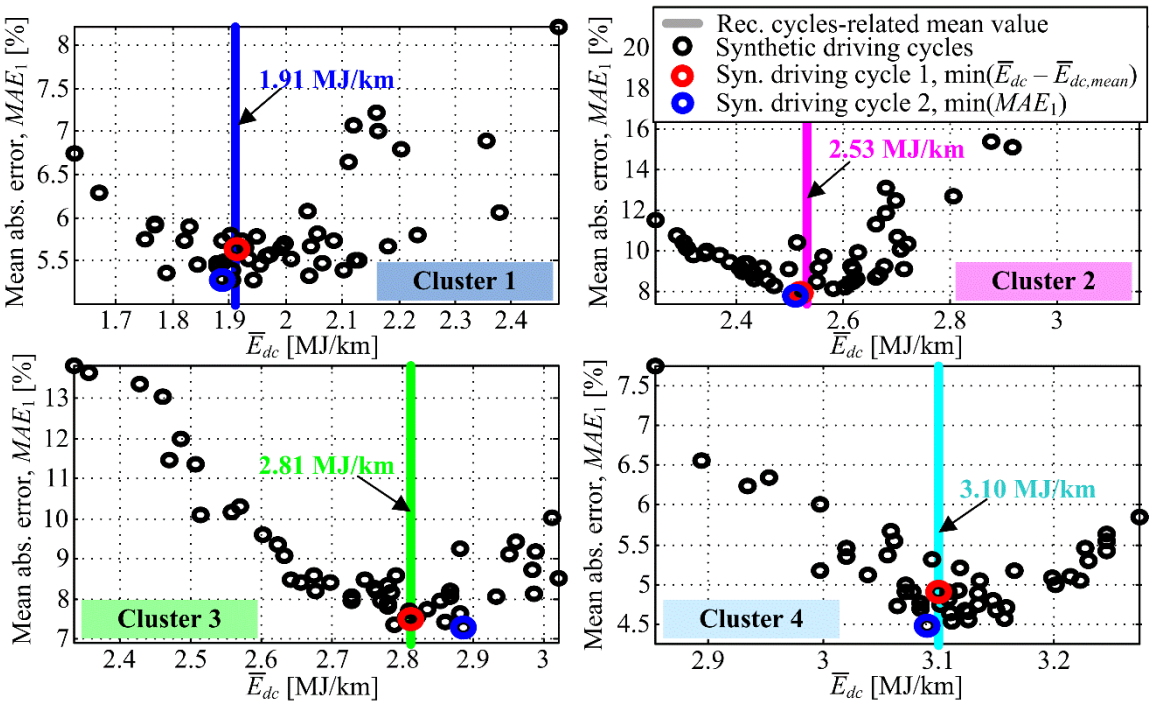

Figure 4: Mean absolute errors of EREV models obtained by using synthetic driving cycles with respect to specific driving cycle energy for different clusters of driving cycles.

Finally, two sets of synthetic driving cycles are selected out of 50 from each cluster for the purpose of transport energy demand modelling. The first set of four synthetic driving cycles (one for each cluster) is selected based on the criterion of minimal deviation of specific energy of synthetic driving cycles from the corresponding mean value for the recorded driving cycles (red circles in Fig. 4 and *Synthetic driving cycle 1* in Table 2). These synthetic driving cycles are shown in Fig. 5. The second set of four synthetic driving cycles is selected based on the criterion of minimal MAE_1 indices (see blue circles in Fig. 4 and *Synthetic*

driving cycle 2 in Table 2). The statistical characteristics related to the duration, travelled distance, mean positive velocity, specific energy, and finally MAE_1 index are given in Table 2 for the selected sets of synthetic driving cycles. Based on these characteristics, it can be concluded that by selecting the synthetic driving cycles which have the specific energy closest to the corresponding mean one for recorded driving cycles, a comparatively low modelling error is obtained and the time-consuming EREV simulations are avoided when compared to the case when the MAE_1 criterion is used to select the driving cycles (5.63% vs. 5.27% for Cluster 1, 7.95% vs. 7.79% for Cluster 2, 7.51% vs. 7.28% for Cluster 3, and 4.90% vs. 4.49% for Cluster 4; see Table 1).

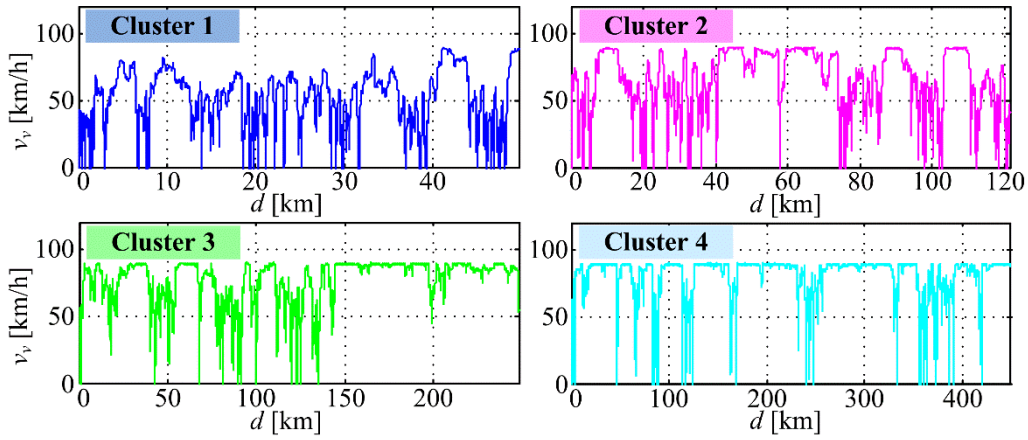

Figure 5: Synthetic driving cycles for each cluster selected/validated according to criterion min($E_{dc} - \overline{E}_{dc}$) (Criterion 1).

Table 2: Basic characteristics of synthetic driving cycles selected for each cluster according to criterion min($E_{dc} - \overline{E}_{dc}$) (Criterion 1) and min(MAE) (Criterion 2).

	Synthetic driving cycle 1					Synthetic driving cycle 2				
	t_{dc} [h]	d [km]	$v_{v,mean}$ [km/h]	$\overline{E}_{dc}$ [MJ/km]	MAE_1 [%]	t_{dc} [h]	d [km]	$v_{v,mean}$ [km/h]	$\overline{E}_{dc}$ [MJ/km]	MAE_1 [%]
Cluster 1	2.1	49.6	37.5	1.91	5.63	2.2	49.6	38.9	1.90	5.27
Cluster 2	3.3	121.4	51.8	2.52	7.95	2.8	121.4	55.0	2.51	7.79
Cluster 3	4.3	247.9	68.7	2.81	7.51	4.1	247.9	70.6	2.89	7.28
Cluster 4	7.2	450.0	72.5	3.10	4.90	6.6	450.0	75.7	3.09	4.49

4 EREV fleet energy demand modelling

This section first provides estimation of all electric range (AER) based on the simulation of EREV model over synthetic driving cycle. Then, transport energy demand models based on EREV simulations over recorded (REC) and synthetic driving cycles (SYN1 and SYN2) are built up. The motivation of using two sets of synthetic driving cycles is to analyse if the synthetic driving cycles selected and validated in a simple way, i.e. according to the specific energy criterion (SYN1; see red circles in Fig. 4) can provide comparable model accuracy as those selected to directly minimise the mean absolute error of model (SYN2; see blue circles in Fig. 4). It should be noted that in the case of validating the SYN1-related driving cycles, the time-consuming EREV model simulations are not needed (only the simple longitudinal vehicle dynamics model is used to calculate the specific driving cycle energy).

4.1 All electric range (AER) estimation

Due to a limited EV range and a relatively long charging period, an accurate estimate of AER is a critical parameter from the perspective of potential EV buyer; for instance an overoptimistic declaration of EV

range can bring a buyer to opt for an EV which cannot satisfy his/her driving needs. The accuracy of an AER estimation based on an EV model predominantly depends on how realistic is the selected driving cycle.

In the case of estimating the AER for the particular EREV model, the synthetic driving cycle whose specific driving cycle energy corresponds to the mean value of all recorded driving cycles (2.77 MJ/km; see Table 1) is selected among 50 generated synthetic driving cycles. It should be emphasized that the synthetic driving cycles generated for this purpose are generated from the TPM parameterised by using all recorded driving cycles (no clustering in this case). Fig. 6 shows the AER values obtained by EREV simulations over all recorded driving cycles (AER_{rec}), their mean values ($AER_{rec,mean}$) and the estimation of 95% confidence intervals ($AER_{rec,mean} \pm 2 \cdot AER_{rec,std}$), and estimation of the AER based on EREV simulation over the selected synthetic driving cycle (AER_{syn}), all for different initial SoC values. Visual inspection of results in Fig. 6 reveals that the AER_{syn} estimations are approximately on the half of AER_{rec} span and aligned with the mean values $AER_{rec,mean}$ for the case of SoC_{init} values between 0.2 and 0.7 (within 10% margins; see Table 3), while they start to deviate slightly from $AER_{rec,mean}$ for SoC_{init} values between 0.8 and 1 (within 15% margins; see Table 3).

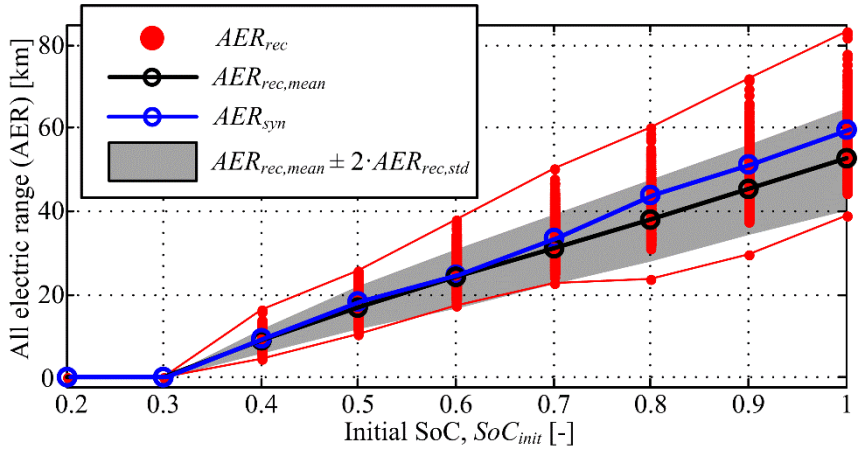

Figure 6: All electric range (AER) with respect to different initial SoC values, obtained by simulating EREV model over synthetic driving cycle and recorded driving cycles.

Table 3: All electric range (AER) for different initial SoC values and for recorded- and synthetic driving cycle-based simulations.

	SoC_{init} [-]								
	0.2	**0.3**	**0.4**	**0.5**	**0.6**	**0.7**	**0.8**	**0.9**	**1**
$AER_{rec,mean}$ [km]	0	0	9.1	17.1	24.1	31.1	38.1	45.6	52.9
AER_{syn} [km]	0	0	9.4	18.4	24.7	33.8	44.1	51.3	59.9
Syn vs. Rec [%]	0	0	+3.2	+7.9	+2.4	+8.7	+15.7	+12.5	+13.1

4.2 EREV fleet energy demand models

From the perspective of EREV and plug-in hybrid electric vehicles (PHEV), the fuel consumption V_f and SoC-at-destination, SoC_{end}, are the variables of interest to be predicted. Since these variables predominantly depend on the initial SoC (SoC_{init}) and the travelled distance d (see Fig. 2b and the corresponding analysis in Section 2), the task of energy demand modelling is to establish the following functional dependences $V_f = f_1(SoC_{init}, d)$, $SoC_{end} = f_2(SoC_{init}, d)$ [2] (similar dependencies are modelled also in [1]).

First, the EREV model is simulated over all recorded driving cycles for the nine discrete levels of initial SoC from Table 3, which resulted in total of 20574 simulations. Then, the obtained V_f vs. (SoC_{init}, d) and SoC_{end} vs. (SoC_{init}, d) points are approximated by two-dimensional 5th order polynomials, whose parameters

are obtained by using Matlab surface fitting tool *sftool*(.) (see Fig. 7). This energy demand model is further referred to as REC.

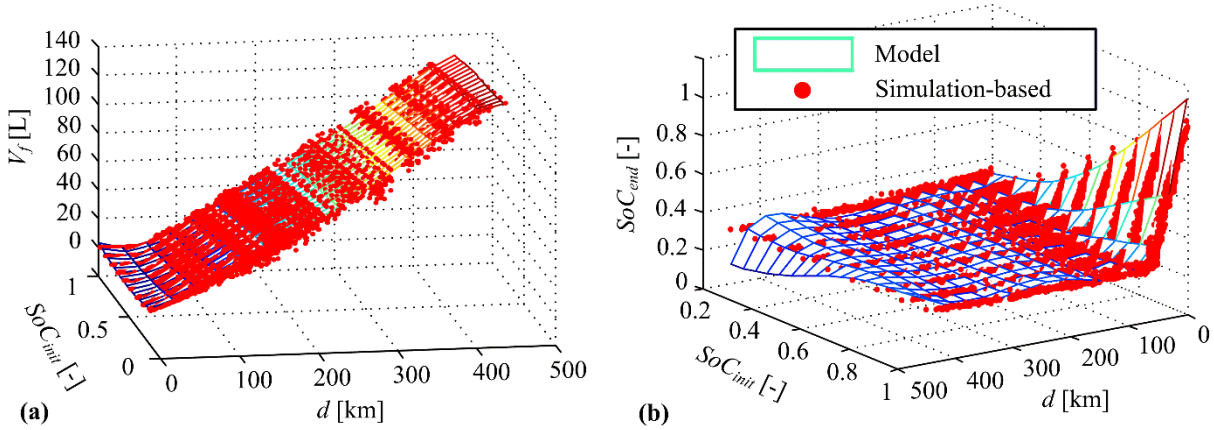

Figure 7: Energy demand model for EREV fleet, related to fuel consumption V_{fuel} (a), and SoC-at-destination SoC_{end} (b), based on two-dimensional 5th order polynomial approximations of the simulation results.

Furthermore, the EREV model is simulated for the two sets of four synthetic driving cycles (each from one cluster, see Fig. 5) for the same nine discrete levels of SoC_{init}, thus resulting in two energy demand models. Total of 36 EREV model simulations are conducted for the case of each set, what is significantly less than in the case of REC model (36 vs. 20574). Different mapping of simulation results are proposed here when compared to the approaches applied in [1, 2], where only values of the final fuel consumption V_f and SoC_{end} at the end of driving cycles were used to build up the energy demand model. These approaches require a larger number of synthetic driving cycles in order to achieve an accurate energy demand model, especially around the bending points where EREV switches from CD to CS regime (see the zoom-in portions of Fig. 8b). However, theoretically an infinite resolution of maps over travelled distance can be obtained by simulating the EREV model over only one (synthetic) driving cycle, since the corresponding simulations result in $V_f(k)$ vs. $d(k)$ and $SoC_{end}(k)$ vs. $d(k)$ (k is the discrete time variable; the approaches from [1, 2] use only $V_f(k_{end})$ and $SoC_{end}(k_{end})$ results for energy demand modelling, where k_{end} represents the final discrete time step, while the approach proposed herein uses the simulation results for all k for energy demand modelling). Since there are four synthetic driving cycles representing the recorded driving cycles from different clusters, the synthetic driving cycle from Cluster 1 is used for modelling of V_f and SoC_{end} for travelled distance $d \in [0, 49.6)$ km, from Cluster 2 for $d \in [49.6, 121.4)$ km, from Cluster 3 for $d \in [121.4, 247.9)$ km, and from Cluster 4 for $d \in [247.9, 450)$ km (see boundaries between clusters in Fig. 3), all for different levels of SoC_{init}. In this way, the number of synthetic driving cycles used for energy demand modelling solely depends on the distribution of recorded specific driving cycle energy, which is shown to be critical for the model accuracy (see results presented in Fig. 4). The model based on Synthetic driving cycles 1 from Table 2 and Fig. 5 is referred to as SYN1, and the model based on Synthetic driving cycles 2 from Table 2 is referred to as SYN2.

Fig. 8 presents the REC, SYN1 and SYN2 models predicting the values of V_f and SoC_{end} with respect to the travelled distance d, for the initial SoC values of 0.3 (solely CS regime) and 1 (CD or combined CD/CS regime). These results point out that REC model can result in non-physical and non-accurate predictions for some SoC_{init} and d input point pairs, e.g. for $SoC_{init} = 1$ and $d \approx 0$ where $SoC_{end} > 1$ and $V_f < 0$ which is not realistic, and for $SoC_{init} = 1$ and $d \approx 65$ km where the bending point is not captured well (Fig. 8b). On the other hand, this is effectively avoided in the case of synthetic driving cycle-based models SYN1 and SYN2, since the simulation results directly (i.e. without approximation) represent energy demand models. By observing the results in Fig. 8, it can be concluded that all models approximate the recorded driving cycles-based data rather well. The detailed comparative numerical analysis of the considered models are given in the next subsection.

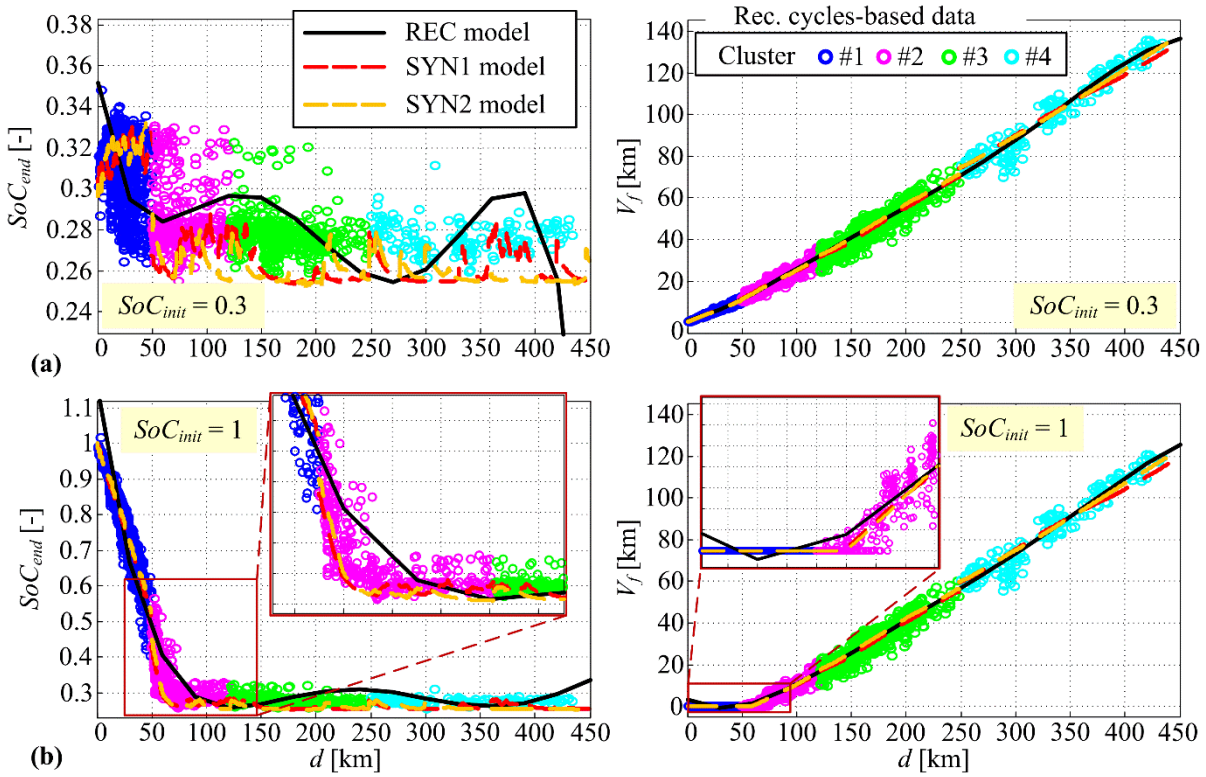

Figure 8: SoC-at-destination SoC_{end} and fuel consumption V_f for the recorded driving cycles and two sets of synthetic driving cycles (see Fig. 4 and Table 2) for the case when initial SoC is SoC_{init} = 0.3 (a) and SoC_{init} = 1 (b).

4.3 Validation of EREV fleet energy demand models

In order to gain insights into the accuracy of the considered energy demand models, the distribution of errors in predicting the SoC-at-destination (ΔSoC_{end}) and the fuel consumption (ΔV_f) for each particular recorded driving cycle are analysed (e.g. ΔV_f represents the difference between the real fuel consumption obtained by the EREV model simulation over recorded driving cycle and the fuel consumption predicted by the corresponding transport demand model; see Fig. 9; ΔV_f and ΔSoC_{end} are normalised and f which corresponds to a probability density function which satisfies the property $\int_{-\infty}^{+\infty} f(t)dt = 1$ is obtained). Fig. 9a reveals that the SoC_{end}-related error distributions of SYN1 and SYN2 models are very similar, and somewhat narrower and slightly biased to the negative errors when compared to that of REC model, while in the case of V_f the error distributions are very similar for the case of all models. The V_f-related error distributions are wider than SoC_{end}-related ones, which means that there is a higher variation of the fuel consumption prediction error than in the case of SoC_{end} predictions. This is reflected through the wider 95% confidence intervals (CFI) and the higher mean absolute errors (MAE) in the case of V_f-related models (see 95% CFI and $MAE_{1,2}$ values in Table 4).

Comparable accuracy of SYN1 and SYN2 models to that of REC model (see 95% CFI and $MAE_{1,2}$ values in Table 4) justifies the energy modelling approach based on synthetic driving cycles and also the validation of synthetic driving cycles based on the single parameter related to the driving cycle specific energy (SYN1 approach; cf. Fig. 4). Furthermore, the total time needed to obtain REC model for this set of recorded driving cycles is 28.4 h (total time column in Table 4). So large total time is is explained by a high number of EREV model simulations, i.e. one per each combination of recorded driving cycle and the level of initial SoC, which resulted in 20574 simulations (2286 recorded driving cycles x 9 initial SoC levels). The total time needed to obtain the synthetic driving cycles-based models (SYN1 and SYN2) is significantly lower and equals to 2.0 h for SYN1 and 2.2 h for SYN2 (Table 4). In the case of SYN1 model, most of the modelling time is used for the calculation of TPM matrix (1.55h which equals to ≈80%), and for generation

of 50x4 synthetic driving cycles needed for driving cycles validation (0.36 h which equals to ≈18%). The rest of time (0.09h which equals to 2%) is used for EREV model simulations (36 in this case, 4 synthetic driving cycles x 9 initial SoC levels). The additional time of 0.2 h in the case of SYN2 model (2.2h vs. 2.0 h) is consumed for additional EREV model simulations over 50x4 synthetic driving cycles for the purpose of synthetic driving cycles validation based on direct minimisation of the modelling error (MAE in Eq. (9); see blue circles in Fig. 4). This is avoided in the case of SYN1 cycles validation, where only the simple longitudinal vehicle dynamic calculations are conducted. However, since the TPM calculation and synthetic driving cycle generation were implemented within Matlab (which consume great majority of the total time), whose code execution could be slower by two orders of magnitude than in C programming language, the total time for TPM calculation and synthetic driving cycles generation can be reduced from ≈2 hours to ≈1 minute if they were implemented in C code.

In summary, the synthetic driving cycle-based energy demand modelling can provide the models of comparative accuracy as those based on simulations over all recorded driving cycles for significantly less time.

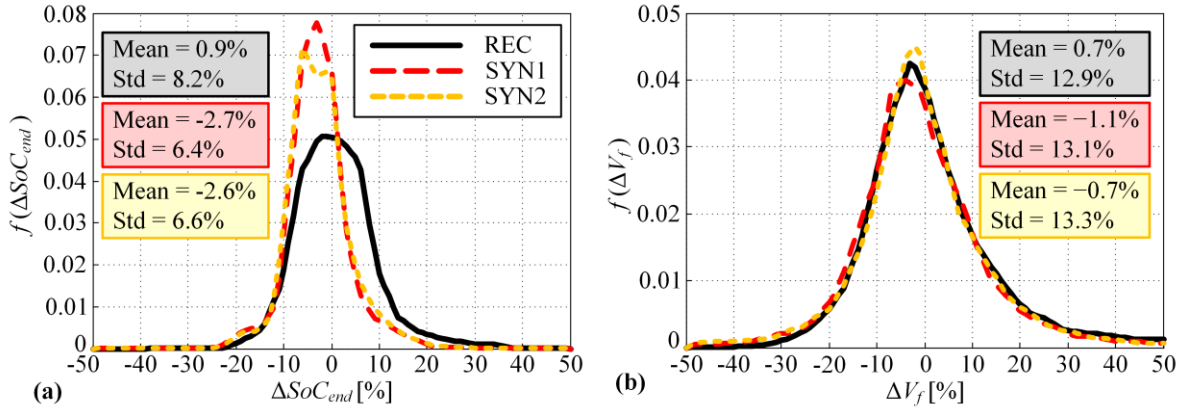

Figure 9: Probability density functions (PDF) of residuals and the corresponding mean values (Mean) and standard deviations (Std) related to models based on recorded driving cycles (REC) and two sets of synthetic driving cycles (SYN1 and SYN2; see Fig. 4 and 5 and Table 2) for SoC-at-destination SoC_{end} (a), and fuel consumption V_{fuel} (b).

Table 4: Number of needed simulations and corresponding execution time values, and validation indices for transport energy demand models obtained by using recorded driving cycles (REC) and synthetic driving cycles (SYN1 and SYN2).

	Number of simulations	**Total time [h]**	**Models**			
			Fuel consumption, V_f		***SoC*-at-destination, SoC_{end}**	
			95% CFI	MAE_1 [%]	95% CFI	MAE_2 [%]
REC	20574 (9x2286)	28.4	[-25.1%, 26.5%]	9.46	[-15.5%, 17.3%]	6.16
SYN1	36 (9x4)	2.0	[-27.3%, 25.1%]	9.77	[-15.5%, 10.1%]	5.24
SYN2	36 (9x4)	2.2	[-27.3%, 25.9%]	9.67	[-15.8%, 10.6%]	5.49

- REC refers to the models obtained from the recorded driving cycles-based EREV simulations
- SYN1 and SYN2 refer to models obtained from the synthetic cycles-based EREV simulations (see Fig. 4 and Table 2 for details about SYN1 and SYN2 cycles)
- 95% CFI corresponds to 95% confidence intervals where 95% of stochastic variable realisations have been fallen; it is estimated as a distribution mean value (Mean) ± 2 standard deviations (2·Std) (see Fig. 9)

5 Conclusion

The methodology of energy demand modelling based on synthetic driving cycles has been presented, including systematic validation of synthetic driving cycles and energy demand models. The presented methodology has been demonstrated for the case of a delivery vehicle fleet of a retail company, consisted of conventional diesel engine-propelled trucks, for which the recorded driving cycles has been available. The conventional trucks are virtually converted to extended range electric vehicles (EREV) of the similar power and torque characteristics, for which the appropriate simulation model has been built. The EREV model is simulated over all recorded driving cycles for different levels of initial battery state-of-charge values SoC_{init}, for the purpose of obtaining recorded data-based energy demand model (REC) and a basis for validation of energy demand models based on synthetic driving cycles (SYN). The recorded driving cycles are separated into clusters, and for each cluster a numerous synthetic driving cycles based on Markov chain-based methodology are generated. Only one synthetic driving cycle is finally selected as a representative for each cluster according to a validation criterion. Two validation criteria have been considered and analysed, one based on the specific driving cycle energy (J/km) for which the time-consuming EREV simulations are not needed (SYN1); and one based on the direct measure of energy model accuracy, which assumes overall EREV model simulations over synthetic driving cycle candidates (SYN2). Finally, the energy demand models REC, SYN1 and SYN2, predicting the fuel consumption (V_f) and the SoC-at-destination (SoC_{end}) based on the initial SoC value (SoC_{init}) and the travelled distance (d), have been validated against the recorded data-based EREV simulation results.

The energy demand analysis results have shown that the specific driving cycle energy is the critical parameter from the perspective of energy demand modelling accuracy, and that the synthetic driving cycles can be validated according to this single validation parameter. Further, it is shown that energy demand models based on synthetic driving cycles are of comparable accuracy as the REC model based on EREV simulations over recorded driving cycles, while their total time consumption is significantly less than in the case of REC model (≈2 hours vs. ≈30 hours). The 95% confidence intervals (CFI), which reflect the energy demand modelling accuracy, are approximately equal to −27% and +26% in the case of the fuel consumption (V_f) prediction errors and for all energy demand models, while in the case of SoC_{end} prediction errors the CFI fall approximately between −16% and +17% for REC model and between −16% and +11% for SYN1 and SYN2 models. The mean absolute error (MAE) in predicting the fuel consumption is approx. 10%, while in the case of predicting SoC_{end} it is approx. 6%. The provided models can be considered to be of satisfying accuracy and can be used within energy planning studies to obtain aggregate energy demands for EV fleets on e.g. national level, within a real-time model predictive-based EV fleet charging optimisation frameworks, etc. The modelling errors would be cancelled in the former case, because the modelling error distributions are closely symmetrical with respect to y-axis (Fig. 9) so that the negative model errors would be cancelled by the positive ones (due to a large number of EVs which are typically considered in this type of studies). In the later case, the impact of modelling errors would be mitigated to some extent by the means of the feedback control loop typically included in the model predictive control approach. However, further reduction of the modelling errors can be achieved by extending the energy demand models by additional input variables, e.g. specific driving cycle energy, geographic positions, which is the subject of the future work.

Acknowledgments

The authors would like to express their gratitude to the company Konzum d.d. for providing the driving cycle data and related technical support.

References

[1] T. K. Lee, Z. S. Filipi, *Response surface modelling approach for the assessment of the PHEV impact on the grid*, 7th IEEE Vehicle Power and Propulsion Conference (VPPC), Chicago, IL, United States, 2011.

[2] B. Škugor, J. Deur, *A bi-level optimisation framework for electric vehicle fleet charging management*, Applied Energy, Vol. 184, pp. 1332-1342, 2016.

[3] T. K. Lee, Z. Filipi, *Synthesis of real-world driving cycles using stochastic process and statistical methodology*, Int. J. Vehicle Design, Vol. 57, No. 1, pp. 17-36, 2011.

[4] B. Škugor, J. Deur, *Delivery vehicle fleet data collection, analysis and naturalistic driving cycles synthesis*, Int. J. of Innovation and Sustainable Development (IJISD), Vol. 10, No. 1, 19-39, 2016.

[5] M. Cipek, B. Škugor, J. Deur, *Comparative Analysis of Conventional and Electric Delivery Vehicles Based on Realistic Driving Cycles*, European Electric Vehicle Congress (EEVC2014), Brussels, Belgium, 2014.

[6] B. Škugor, M. Cipek, D. Pavković, J. Deur, *Design of a power-split hybrid electric vehicle control system utilizing a rule-based controller and an equivalent consumption minimization strategy*, Proceedings of the Institution of Mechanical Engineers, Part D, Journal of Automobile Engineering, Vol. 228, No. 6, pp. 631-648, 2014.

[7] B. Škugor, M. Cipek, J. Deur, *Control Variables Optimization and Feedback Control Strategy Design for the Blended Operating Mode of an Extended Range Electric Vehicle*, SAE International Journal of Alternative Powertrains, SAE paper # 2014-01-1898, Vol. 3, No. 1, pp. 152-162., 2014.

Authors

Branimir Škugor is a postdoctoral researcher at the University of Zagreb-FMENA. He received his Ph.D. degree in Mechanical Engineering from the same university in 2016. He has participated on one project supported by the Croatian Science Foundation and two projects supported by the Ford Motor Company. His research interests include: advanced control of hybrid electric vehicles powertrain, modelling and charging control of electric vehicle fleets, and analysis and synthesis of driving cycles.

Joško Deur is a Full Professor at the University of Zagreb, where he teaches courses in electrical machines and servo-drives, digital control systems, and automotive mechatronics. In 2000, he was a guest researcher at the Ford Research Laboratory, Dearborn, MI. Subsequently, professor Deur has led numerous projects including those supported by Ford Motor Company and Jaguar Cars Ltd. His research interests include: modelling and control of vehicle mechatronic systems, hybrid electric vehicles, optimisation and optimal control, electrical energy storage systems, e-mobility, and servo-systems.